Electronic Supplementary Information (ESI)

Lipid droplet targeting-guided hypoxic photodynamic therapy with curcumin analogs

Xuewei Li,[ab] Weimin Liu, *[ab] Xiuli Zheng,[ac] Meiyu Jiang,[ab] Yimin Guo,[ab] Jie Sha,[ab] Jiasheng Wu,[a] Haohui Ren,[ac] Honglei Gao,[ab] Shuai Wang,[ab] and Pengfei Wang *[ab]

[a]*Key Laboratory of Photochemical Conversion and Optoelectronic Materials and CityU-CAS Joint Laboratory of Functional Materials and Devices, Technical Institute of Physics and Chemistry, Chinese Academy of Sciences, Beijing, 100190, People's Republic of China.*

[b]*School of Future Technology, University of Chinese Academy of Sciences, Beijing, 100049, People's Republic of China.*

[c]*Institute of Optical Physics and Engineering Technology, Qilu Zhongke, Jinan, 250000, People's Republic of China.*

**Email: wmliu@mail.ipc.ac.cn; wangpf@mail.ipc.ac.cn*

1. Materials and methods

Phosphate buffer solution (PBS), BODIPY 493/503 (BODIPY), Mito-tracker Green (MTG), Lyso-tracker Green (LTG), 9,10-anthracenediyl-bis (methylene) dimalonic acid (ABDA), singlet oxygen sensor Green (SOSG), Rose Bengal (RB), Dihydroethidium (DHE), 2',7'-dichlorodihydrofluorescein diacetate (DCFH-DA), calcein AM and propidium iodide (AM/PI), and thiazolyl blue tetrazolium bromide (MTT) were purchased from Innochem, jkchemical, Sigma-Aldrich, or Beijing Solarbio Technology Company. All solvents and inorganic salts were purchased from Beijing Reagent, Sinopharm Chemical Reagent Beijing or General-Reagent, and used without further purification. HepG-2 (human hepatocarcinoma cell line), HeLa (human cervical adenocarcinoma epithelial cell line), and 4T1 (mouse breast cancer cell line) were obtained from the Center of Cells, Peking Union Medical College.

^{1}H nuclear magnetic resonance (NMR) and ^{13}C NMR spectra were performed on Bruker Avance 400 and 600 MHz spectrometers, respectively. Mass spectrometry (MS) was performed on an Accurate-Mass Q-TOF LC/MS, Agilent Technologies 6530 system. A Hitachi U-3900 ultraviolet-visible (UV-Vis) spectrophotometer was utilized for UV-Vis absorption spectra detection, and the fluorescence experiments were recorded using a Hitachi F-4600 spectrofluorimeter. Cell imaging was captured by a Nikon C1-Si confocal laser scanning microscope (CLSM).

2. Theoretical calculations

To study the molecular geometry, we determined the lowest un-occupied molecular orbital (LUMO) and highest occupied molecule orbital (HOMO) distributions of CUR, CCOH and CCN, and performed density functional theory (DFT) calculations on the basis of B3LYP/6-31G*.

3. Syntheses of compounds 1, 2, 3, 4, CCOH and CCN.

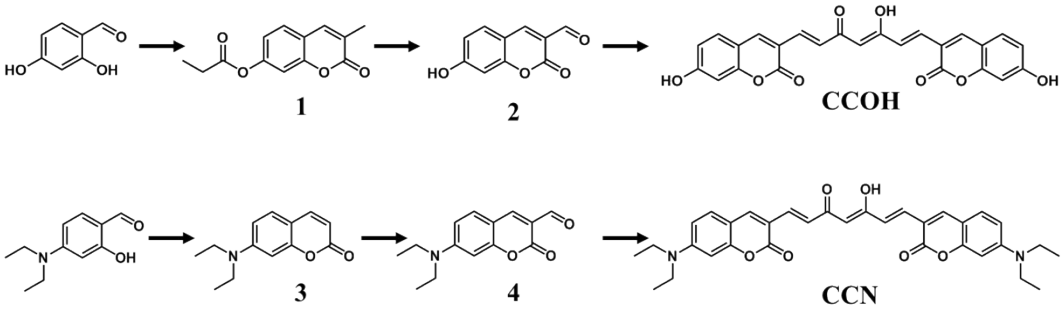

Fig. S1 synthetic route of CCOH and CCN.

Compounds 1-4 were synthesized according to previously reported procedures.[1, 2]

Synthesis of compound 3-methyl-2-oxo-2H-chromen-7-yl propionate (1):

2,4-Dihydroxybenzaldehyde (7 g, 50 mmol) and sodium propionate (10.5 g, 110 mmol) were dissolved in propionic anhydride (80 ml), piperidine (2 ml) was added dropwise, and the mixture was stirred under reflux for 3 h. Cooled to room temperature, solution was poured into a beaker containing ice water (100 ml), and stirred at room temperature for 30 min. Then, filtered under reduced pressure to obtain a white crude product, and recrystallized in ethanol to obtain white needle-like crystals 1 (7 g, 58.1%). ^{1}H NMR (400 MHz, $CDCl_3$, δ): 7.49 (s, 1H), 7.40 (d, 1H), 7.07 (s, 1H), 7.01(d, 1H), 2.62 (q, 2H), 2.19 (s, 3H), 1.27 (q, 3H).

Synthesis of compound 7-hydroxy-2-oxo-2H-chromene-3-carbaldehyde (2):

Compound 1 (3.6 g, 15 mmol) and N-Bromosuccinimide (7.2 g, 40 mmol) were poured into a 100 ml double-

neck flask. CCl_4 (50 ml) and a constant amount of AIBN were added under N_2 atmosphere, which was stirred under reflux for 24 h. After cooling to room temperature, the crude product was obtained by filtration under reduced pressure, which was washed three times with CCl_4. The above product and sodium acetate (11 g, 133.5 mmol) were dissolved in glacial acetic acid (75 ml), and stirred at reflux for 12 h. After cooled to room temperature, HCl (2M, 50 ml) was added and stirred at room temperature overnight. The solution was spin-dried under reduced pressure, and compound 2 (1.1 g, 41%) was obtained by column chromatography. ^{1}H NMR (400 MHz, DMSO-d_6, δ): 11.32 (s, 1H), 9.96 (s, 1H), 8.59 (s, 1H), 7.82 (d, 1H), 6.89-6.86 (m, 1H), 6.78 (s, 1H).

Synthesis of compound 3,3'-((1E,3Z,6E)-3-hydroxy-5-oxohepta-1,3,6-triene-1,7-diyl)bis(7-hydroxy-2H-chromen-2-one) (CCOH):

Boron trioxide (700 mg, 10 mmol) was dissolved in anhydrous N, N-Dimethylformamide (DMF) (10ml) under nitrogen atmosphere, the temperature was raised to 120 °C and the mixture was stirred for 10 min. Then acetylacetone (0.11 ml, 1 mmol), tributyl borate (0.54 ml, 2 mmol), compound 2 (460 mg, 2.4 mmol), and 1, 2, 3, 4-tetrahydroquinoline (0.1 ml) were successively added, and the resulting mixture was stirred at 120° C for 8 h. After cooling to room temperature, extraction was performed with ethyl acetate, and the extract was washed with ultrapure water. Finally, an orange solid (CCOH) (190 mg, 43%) was obtained by silica gel column purification.^{1}H NMR (400 MHz, DMSO-d_6, δ): 16.08 (s, 1H), 10.94 (s, 2H), 8.41 (s, 2H), 7.61 (d, 2H), 7.56 (d, 2H), 7.22 (d, 2H), 6.87 (d, 2H), 6.76 (s, 2H), 6.20 (s, 1H). ^{13}C NMR (150 MHz, DMSO-d_6, δ): 183.09, 162.85, 159.21, 155.32, 145.29, 135.27, 130.87, 125.87, 116.96, 114.05, 111.77, 102.39, 101.96. $[M + H]^+$ calcd for $C_{25}H_{16}O_8$, 445.0845, found: 445.0842.

Synthesis of compound 7-(diethylamino)-2H-chromen-2-one (3):

2, 4-dihydroxybenzaldehyde (3.86 g, 20 mmol) was dissolve in anhydrous ethanol (100 ml), diethyl malonate (6.6 ml, 43 mmol) and piperidine (4 ml) were added. The reaction under reflux for 4h and cooled to room temperature to obtain a reddish-brown viscous liquid. The reddish-brown viscous liquid was transferred to a 250 ml two-necked flask, concentrated hydrochloric acid (40 ml) and glacial acetic acid (40 ml) were added, and the mixture was heated to reflux for 8 h. After cooled to room temperature, the solution was transferred to ice water (100 ml). Aqueous NaOH solution was used to adjust to neutral pH, which was filtered with suction, and the solid was washed three times with ultrapure water and ethanol to obtain khaki solid 3 (3.4 g, 78%). ^{1}H NMR (400 MHz, $CDCl_3$, δ): 7.55 (d, 1H), 7.23 (d, 1H), 6.59 (d, 1H), 6.51 (s, 1H), 6.06 (d, 1H,), 3.42 (m , 4H), 1.21 (t, 6H).

Synthesis of compound 7-(diethylamino)-2-oxo-2H-chromene-3-carbaldehyde (4):

Phosphorus oxychloride (5 ml) and anhydrous DMF (6 ml) were added dropwise to a double-necked flask, and the temperature was raised to 50 °C and stirred for 0.5 h. The DMF solution containing compound 3 (3.3 g, 15 mmol) was transferred into a two-necked flask and reacted at 60 °C for 12 h. The reaction solution was cooled to room temperature and added into ice water (100 ml), Aqueous NaOH solution was used to adjust to neutral pH, which was filtered with suction and washed the solid three times with ultrapure water and ethanol. Ethanol was used to obtain orange needle-like crystalline solid 4 (2.9 g, 75%). ^{1}H NMR (400 MHz, $CDCl_3$, δ): 10.13 (s, 1H), 8.26 (s, 1H), 7.43 (d, 1H), 6.67 (d, 1H), 6.50 (s, 1H), 3.49 (m, 4H), 1.25 (t, 6H).

Synthesis of compound 3,3'-((1E,3Z,6E)-3-hydroxy-5-oxohepta-1,3,6-triene-1,7-diyl)bis(7-(diethylamino)-

2H-chromen-2-one) (CCN)：

Boron trioxide (700 mg, 10 mmol) in anhydrous DMF (10 ml) under nitrogen atmosphere, the temperature was raised to 120 °C and the mixture was stirred for 10 min. Then acetylacetone (0.11 ml, 1 mmol), tributyl borate (0.54 ml, 2 mmol), compound 4 (590 mg, 2.4 mmol), and 1, 2, 3, 4-tetrahydroquinoline (0.1 ml) were successively added, and the resulting mixture was stirred at 120°C for 3 h. After cooling to room temperature, extraction was performed with dichloromethane, and the extract was washed with ultrapure water. Finally, a red brown solid (CCN) (350 mg, 63%) was obtained by silica gel-column purification. ^{1}H NMR (400 MHz, $CDCl_3$, δ): 16.02 (s, 1H), 7.71 (s, 2H), 7.51 (d, 2H), 7.33 (d, 2H), 7.23 (d, 2H), 6.64 (d, 2H), 6.52 (s, 2H), 5.86 (s, 1H), 3.47-3.42 (m, 8H), 1.24 (t, 12H). ^{13}C NMR (150 MHz, $CDCl_3$, δ): 183.49, 160.27, 156.38, 151.41, 144.25, 135.37, 129.83, 125.73, 115.51, 109.66, 109.22, 103.32, 97.24, 45.20, 12.46. $[M + H]^+$ calcd for $C_{25}H_{16}O_8$, 555.2417, found: 555.2246.

4. Photophysical properties

Methods for detecting $O_2^{-\cdot}$ are reported.[3] CUR, CCOH, and CCN (20 μL, 1 mmol L^{-1} in DMSO), DHE (20 μL, 1 mmol L^{-1} in DMSO) and ctDNA (20 μL, 2 mg mL^{-1} in H_2O) were added to PBS (pH = 7.4, 1 mL). The mixture was irradiated with xenon lamp (0.05 W cm^{-2}) or 532 nm laser (0.02 W cm^{-2}) respectively, and the fluorescence spectra (excitation at 510 nm) of the solution were recorded every minute.

To evaluate the $^{1}O_2$ quantum yield under the irradiation of xenon lamp. [4] RB was used as a standard photosensitizer for $^{1}O_2$ production and ABDA was used as a singlet oxygen trapping agent. The maximum absorption wavelength of CUR, CCOH, and CCN to about 0.2 OD in PBS (pH = 7.4, 2 mL). ABDA solution (40 μL, 1 mg mL^{-1} in DMSO) were added to the solution. The mixture was irradiated with a xenon lamp (0.05 W cm^{-2}), and the OD values were recorded at 378 nm every one min by using a UV-Vis spectrophotometer. The $^{1}O_2$ quantum yield of the CUR, CCOH and CCN were calculated using the following formula:

$$\Phi_{PS} = \Phi_{RB}\frac{K_{PS}A_{RB}}{K_{RB}A_{PS}}$$

Where PS stands for one of CUR, CCOH or CCN. K_{PS} and K_{RB} are the decomposition rate constants of ADBA by the PS and RB, respectively. A_{PS} and A_{RB} represent the light absorbed by the PS and RB, respectively, which were determined by integration of the optical absorption bands in the wavelength range 400–700 nm. Φ_{RB} is the $^{1}O_2$ quantum yield of RB, and Φ_{RB}= 0.75 in water.

To evaluate the $^{1}O_2$ quantum yield of CCN under the irradiation of 532nm laser. The absorption in 532 nm of RB and CCN were adjusted to 0.2 OD in PBS (pH = 7.4, 2 mL). ABDA solution (40 μL, 1 mg mL^{-1} in DMSO) was added to the PBS with RB or CCN. The mixture was irradiated with 532 nm laser (0.01 W cm^{-2}), and the OD values were recorded at 378 nm every one min. The $^{1}O_2$ quantum yield of CCN were calculated using the following formula:

$$\Phi_{CCN} = \Phi_{RB}\frac{K_{CCN}}{K_{RB}}$$

Where K_{CCN} and K_{RB} are the decomposition rate constants of ADBA by the CCN and RB, respectively. Φ_{RB} is the $^{1}O_2$ quantum yield of RB, and Φ_{RB}= 0.75 in water.

SOSG was used as a probe for $^{1}O_2$ production. [5] CUR, CCOH, and CCN (20 μL, 1 mmol L^{-1} in DMSO), SOSG (2 μL, 1 mmol L^{-1} in MeOH) were added to PBS (pH = 7.4, 1 mL). The mixture was irradiated (532 nm, 0.05 W cm^{-2}), and the fluorescence spectra (excitation at 504 nm) of the solution were recorded every minute.

To evaluate the production of active oxygen in 532nm laser, variable temperature electron spin resonance spectroscopy (ESR). All samples were irradiated with a 532 nm laser (0.01 W cm^{-2}), and the ESR signal spectrum were recorded before and after laser irradiation.

Test for photostability in solution: record the OD value of CCN (2 mL, 5 μmol L^{-1} in DMSO) under laser (532 nm, 0.05 W cm^{-2}) irradiation every minute.

Testing pH stability in PBS: CCN (20 μL, 1 mmol L^{-1} in DMSO) were added to 1.5 mL PBS (pH = 3.0, 4.0, 5.0, 6.0, 7.0, 8.0, 9.0, 10.0).

5. Cellular co-localization and photostability experiments

HepG-2, HeLa, and 4T1 cells were incubated with CCN (2 μmol L^{-1}) for 1 h, washed thrice with PBS, and then the cells were incubated with BODIPY (0.5 μmol L^{-1}), MTG (0.2 μmol L^{-1}) or LTG (0.2 μmol L^{-1}) for 10 min. The organelle-targeted fluorescent probe and CCN were collected in two channels, namely, the 488 nm laser excitation collected with 500−530 nm and 568−643 nm band passes.

HepG-2 cells were incubated with CCN (2 μmol L^{-1}) and BODIPY (0.5 μmol L^{-1}), and 40 consecutive images were captured in 10 min through CLSM. The change in fluorescence intensity was recorded.

6. Detection of $O_2^{-\bullet}$ and $^1O_2$ in cells

DHE was used as a probe to examine the production of $O_2^{-\bullet}$ in live cells. HepG-2 cells were incubated with CCN (2 μmol L^{-1}) for 1 h and added with DHE (10 μmol L^{-1}) for 30 min. The cells were irradiated with a 532 nm laser (0.02 W cm^{-2}) for 1 min, and confocal imaging was performed. The control group was added with DHE or CCN with laser (0.02 W cm^{-2}). DHE was excited by 488 nm laser and imaged in the 568–643 nm channels.

SOSG was used as a probe to examine the production of $^1O_2$ in live cells. After the incubation with CCN (2 μmol L^{-1}) for 1 h, HepG-2 cells were fixed with ice methanol for 3 min and added with SOSG (5 μmol L^{-1}) for 30 min. The HepG-2 cells were irradiated with a 532 nm laser (0.02 w cm^{-2}) for 1 min, and confocal imaging was performed. The control group was added SOSG or CCN with laser (0.02 W cm^{-2}). The signals of SOSG in the 500−530 nm channel were acquired under a confocal microscope.

7. Detection of ROS in OA

CCN (2 μl, 1 mmol L^{-1}) was dissolved in 1ml OA, and DCFH-DA (2 μl, 1 mmol L^{-1}) was dissolved in 1ml PBS. A distinct boundary was observed between the water and oil phases. The mixture was irradiated with a 532 nm laser (0.01 W cm^{-2}), and the fluorescence spectra (excitation at 477 nm) of the solution were recorded every 5 min.

8. Monitoring LDs changes during PDT

HepG-2 cells incubated with CCN (5 μmol L^{-1}) were irradiated with a 532 nm laser (0.02 W cm^{-2}) for 16 min. The pictures were taken every 4 min through CLSM to observe the changes in cell status and intracellular LDs. The control group underwent the same operation without laser.

9. MTT assay and in vitro PDT

The anti-cancer capability of CCN in HepG-2, HeLa, and 4T1 cells was evaluated by the MTT method. Cells were incubated with different concentrations of CCN. The medium was replased and irradiated with a 532 nm laser (0.1 W cm^{-2}, for 10 min). After 24 h, 20 μL MTT (5 mg mL^{-1} in PBS) was added and incubated with the cells for 4 h. The medium was poured out, and 80 μL dimethyl sulfoxide (DMSO) was added. The absorbance was measured

at 570 nm. The hypoxic group was placed in a hypoxic bag for irradiation. The operation of dark toxicity experiment was the same as that of light toxicity experiment but without the use of laser.

To investigate the photodynamic effect on cells, we utilized AM/PI as a probe for live or dead cell imaging. HepG-2 cells irradiated by laser only and incubated with CCN (2.5 μmol L^{-1}) alone were set as the control group. HepG-2 cells were treated with CCN (2.5 μmol L^{-1}) for 1 h and irradiated with a 532 nm laser (0.1 W cm^{-2}) for 10 min. After 24 h incubation, the HepG-2 cells were co-stained with AM/PI for 30 min and imaged under a confocal microscope. AM/PI were excited by 488 nm laser, and the signals were collected in the 500-530 nm and 568-643 nm bands, respectively.

10. Supplementary Spectra and charts

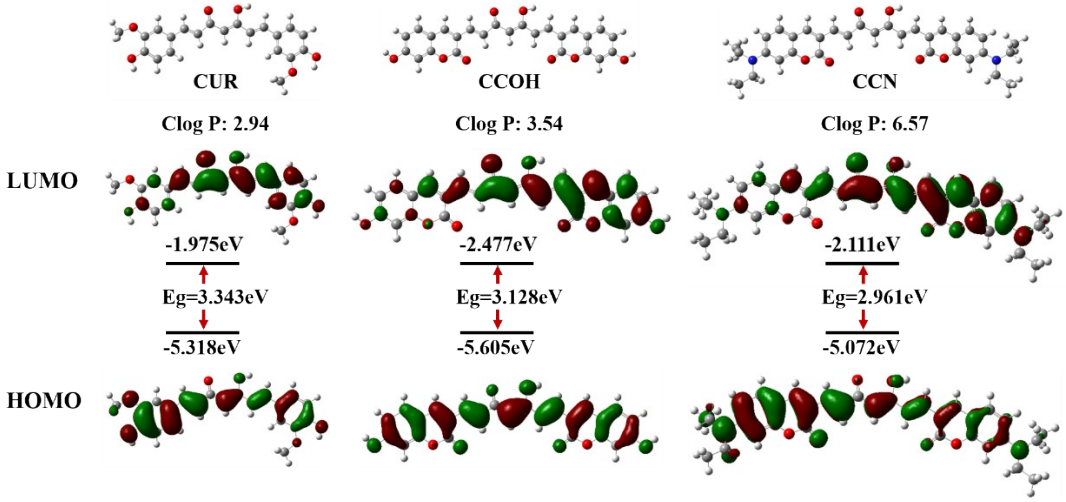

Fig. S2 DFT simulation of HOMO and LUMO energy levels and Clog P of CUR, CCOH and CCN.

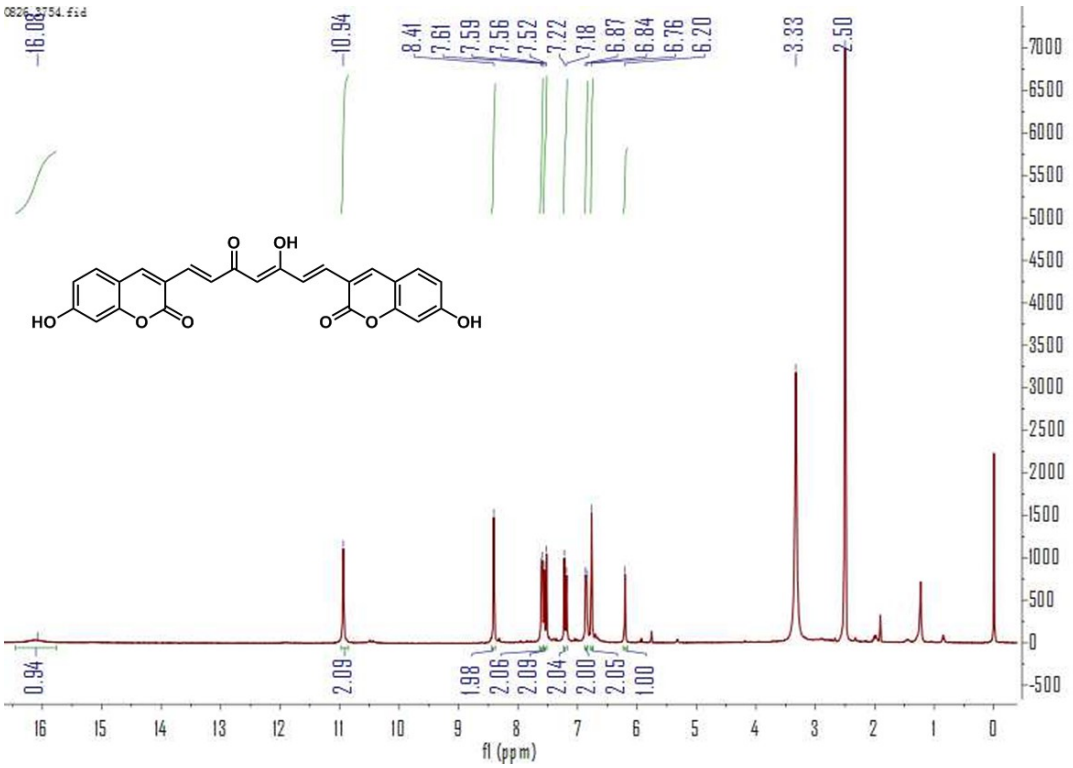

Fig. S3 The ^{1}H NMR spectrum of CCOH in DMSO-d_6.

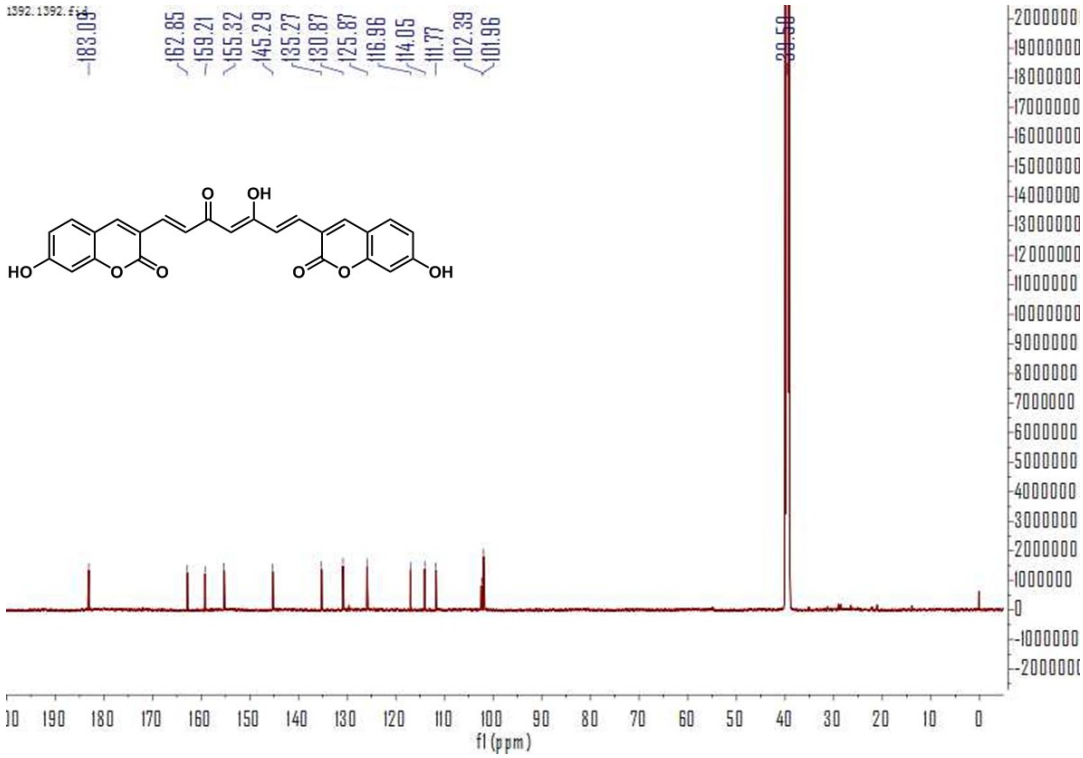

Fig. S4 The ^{13}C NMR spectrum of CCOH in DMSO-d_6.

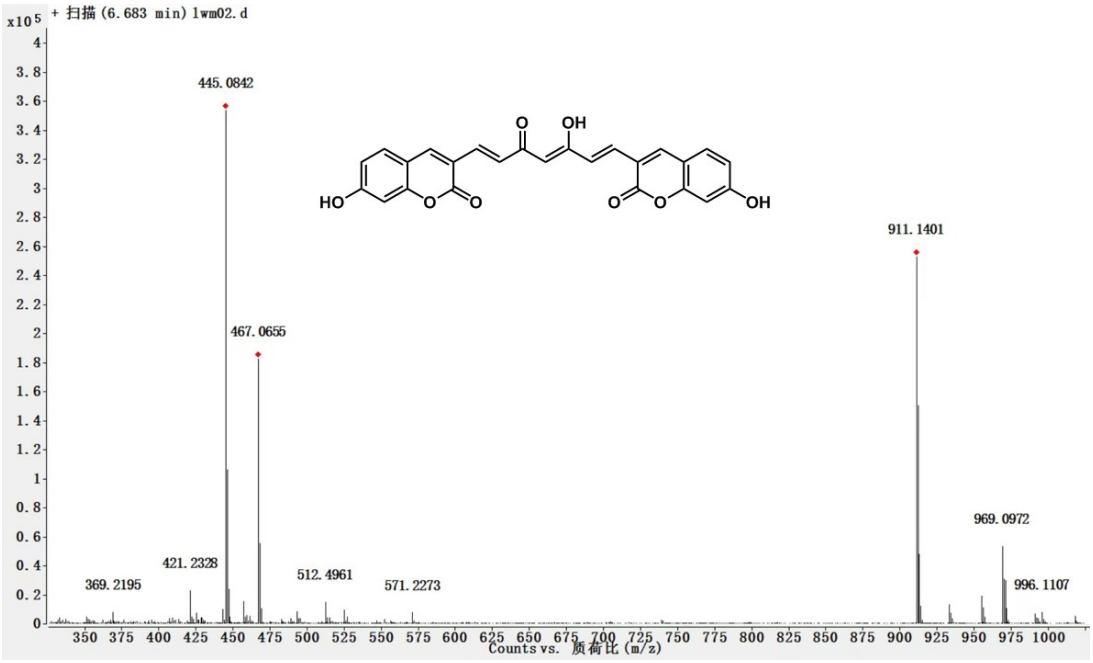

Figure. S5 ES-MS spectra of CCOH.

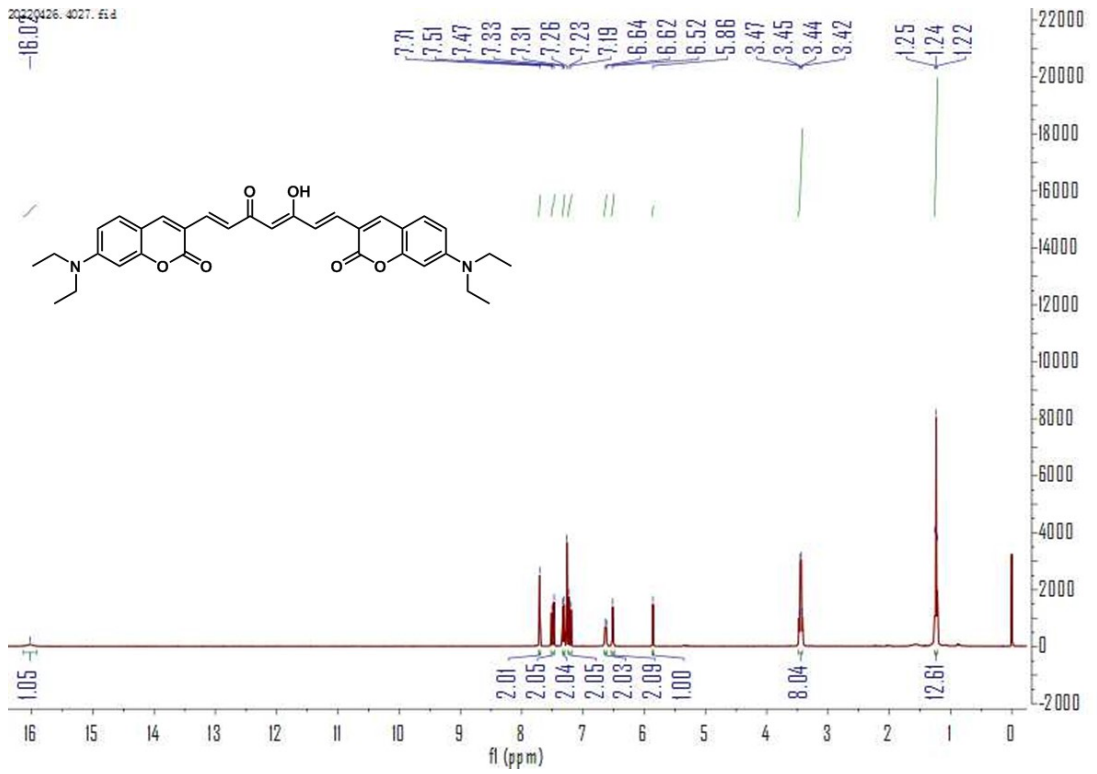

Fig. S6 The ^{1}H NMR spectrum of CCN in $CDCl_3$.

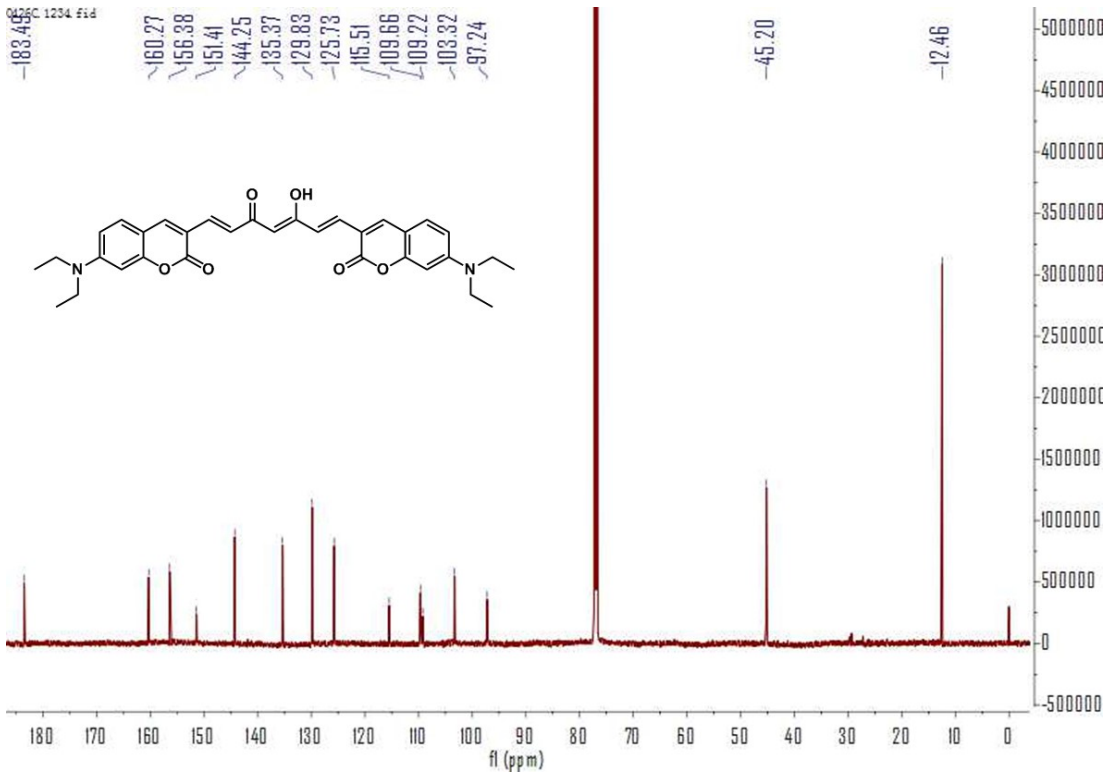

Fig. S7 The ^{13}C NMR spectrum of CCN in $CDCl_3$.

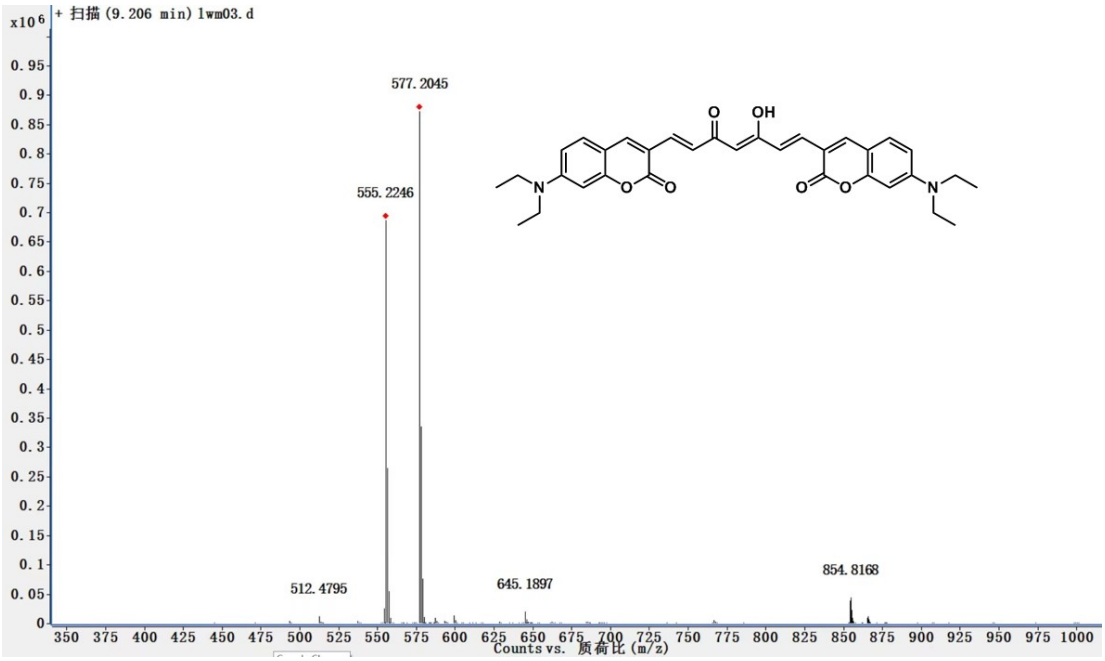

Figure. S8 ES-MS spectra of CCN.

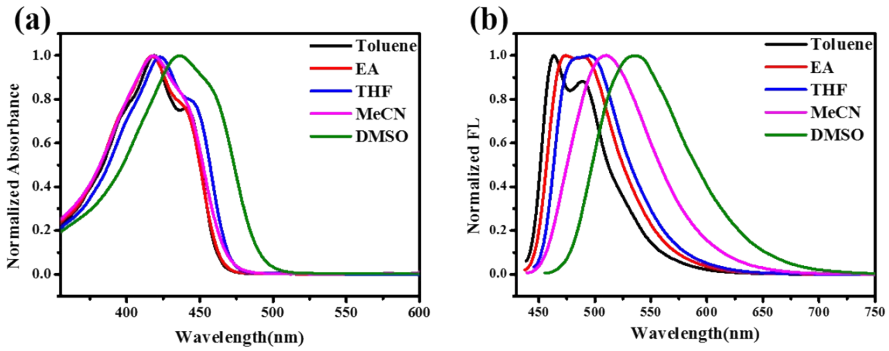

Fig. S9 (a) Normalized absorption spectra and (b) Normalized fluorescence spectra of CUR in Toluene (λ_{ex}=418nm), EA (λ_{ex}=417nm), THF (λ_{ex}=423nm), MeCN (λ_{ex}=419nm) and DMSO (λ_{ex}=435nm).

Table S1 Photophysical properties of CUR in Toluene, EA, THF, MeCN and DMSO.

	$\lambda_{abs\ max}$ (nm)	$\lambda_{em\ max}$ (nm)	PLQY	Stokes Shift （nm）	ε ($M^{-1}cm^{-1}$)
Toluene	418,442	463,490	0.083	72	27900
EA	417	473,492	0.135	75	55500
THF	423	495	0.174	72	60400
MeCN	419	510	0.188	91	53400
DMSO	435	536	0.068	101	51200

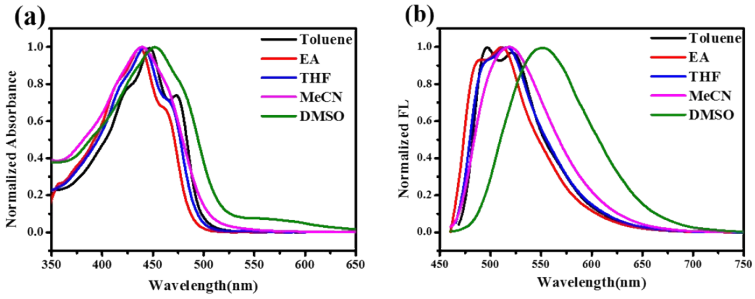

Fig. S10 (a) Normalized absorption spectra and (b) Normalized fluorescence spectra of CCOH in Toluene (1%DMSO) (λ_{ex}=448nm), EA (λ_{ex}=440nm), THF (λ_{ex}=442nm), MeCN (λ_{ex}=439nm) and DMSO (λ_{ex}=451nm).

Table S2 Photophysical properties of CCOH in Toluene (1%DMSO), EA, THF, MeCN and DMSO.

	λ_{abs}^{max} (nm)	λ_{em}^{max} (nm)	PLQY	Stokes Shift （nm）	ε ($M^{-1}cm^{-1}$)
Toluene (1%DMSO)	448, 474	496,524	0.366	76	42000
EA	440	486,512	0.267	72	58200
THF	442	511	0.306	69	61500
MeCN	439	520	0.269	82	55500
DMSO	451	549	0.111	98	51300

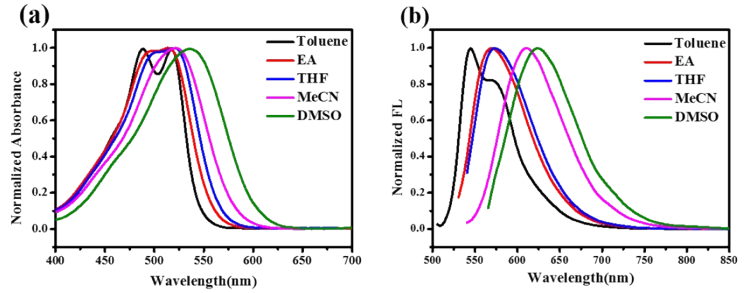

Fig. S11 (a) Normalized absorption spectra and (b) Normalized fluorescence spectra of CCN in Toluene (λ_{ex}=485nm), EA (λ_{ex}=510nm), THF (λ_{ex}=520nm), MeCN (λ_{ex}=521nm) and DMSO (λ_{ex}=537nm).

Table S3 Photophysical properties of CCN in Toluene, EA, THF, MeCN and DMSO.

	$\lambda_{abs\ max}$ (nm)	$\lambda_{em\ max}$ (nm)	PLQY	Stokes Shift （nm）	ε $M^{-1}cm^{-1}$
Toluene	485, 515	545，575	0.630	60	62400
EA	510	570	0.619	60	54600
THF	520	585	0.628	65	103000
MeCN	521	612	0.120	91	46000
DMSO	537	625	0.073	88	72000

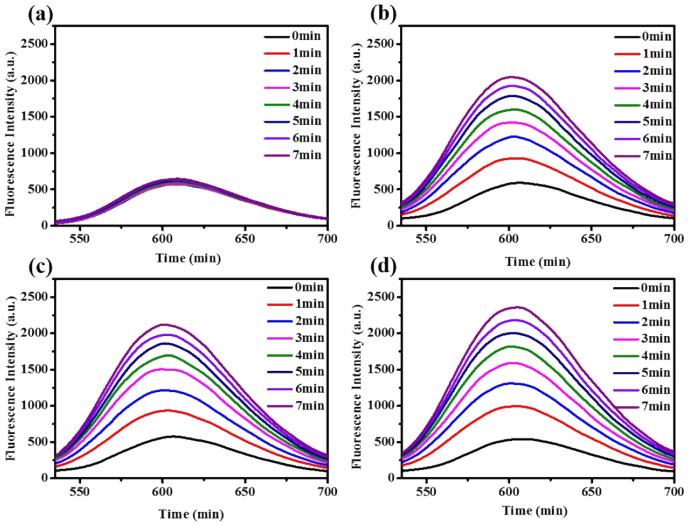

Fig. S12 Fluorescence spectra of DHE (λ_{ex}: 510 nm) in PBS under Xenon lamp irradiation (0.05 W cm^{-2}) of (a) only DHE (20 μM), (b) CUR (20 μM), (c) CCOH (20 μM), and (d) CCN (20 μM).

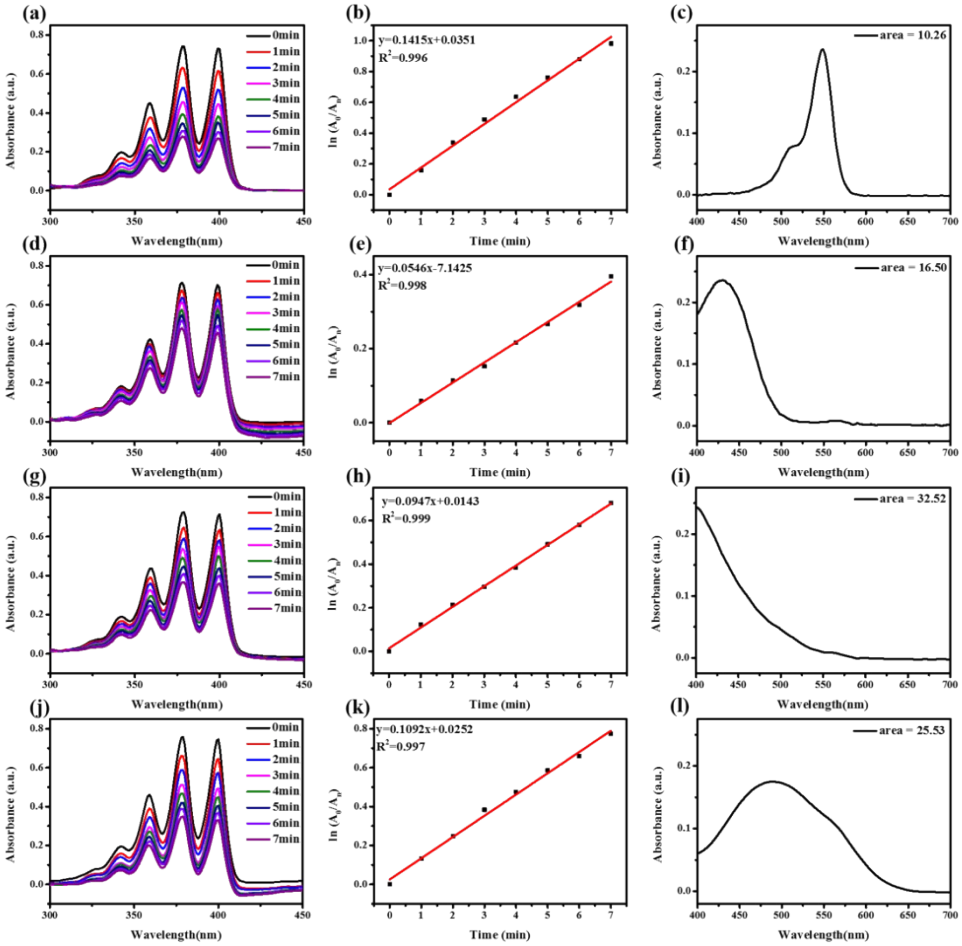

Fig. S13 UV-Vis spectra of ABDA (20 μM) in PBS under white light irradiation (0.05 W cm^{-2}) in the presence of (a) RB, (d) CUR, (g) CCOH and (j) CCN. The absorbance decay of the ADBA at 378 nm under white light irradiation (0.05 W cm^{-2}) in the presence of (b) RB, (e) CUR, (h) CCOH, and (k) CCN. The absorption spectrum in 400–700 nm of (c) RB, (f) CUR, (i) CCOH, and (l) CCN.

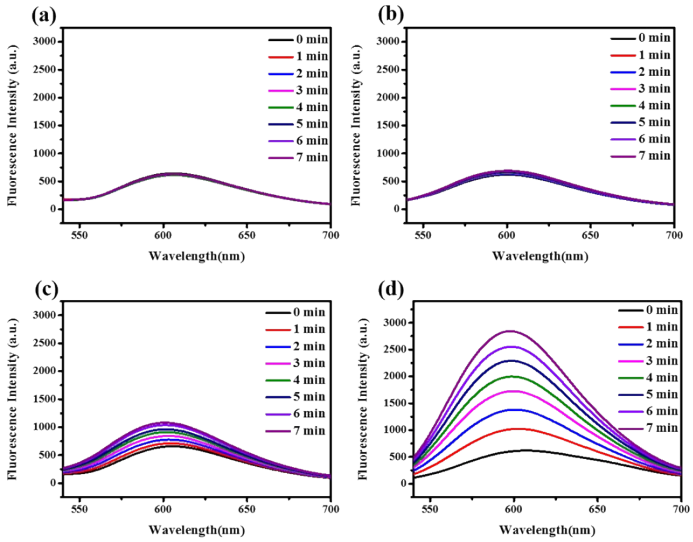

Fig. S14 Fluorescence spectra of DHE (λ_{ex}: 510 nm) in PBS under laser irradiation (532 nm, 0.02 W cm^{-2}) of (a) only DHE (20 μM), (b) CUR (20 μM), (c) CCOH (20 μM), and (d) CCN (20 μM).

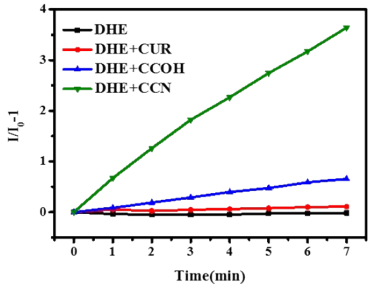

Fig. S15 Relative changes of fluorescence emission intensity at 610 nm of DHE (λ_{ex}: 510 nm) in the presence of CUR (20 μM), CCOH (20 μM), and CCN (20 μM) under laser irradiation (532 nm, 0.02 W cm^{-2}).

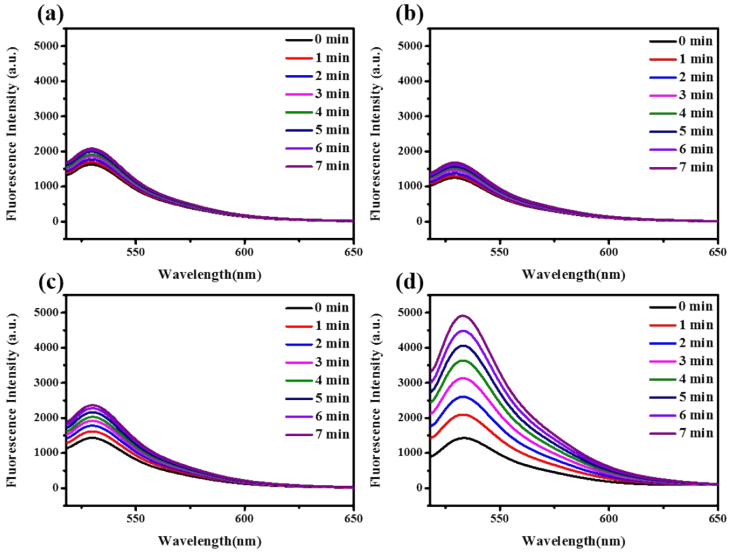

Fig. S16 Fluorescence spectra of SOSG (λ_{ex}: 504 nm) in PBS under laser irradiation (532 nm, 0.05 W cm^{-2}) of (a) only SOSG (20 μM), (b) CUR (20 μM), (c) CCOH (20 μM), and (d) CCN (20 μM).

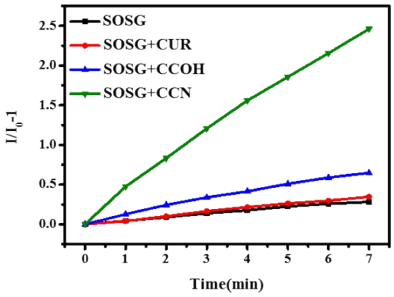

Fig. S17 Relative changes of fluorescence emission intensity at 532 nm of SOSG (λex: 504 nm) in the presence of CUR (20 μM), CCOH (20 μM), and CCN (20 μM) under laser irradiation (532 nm, 0.05 W cm^{-2}).

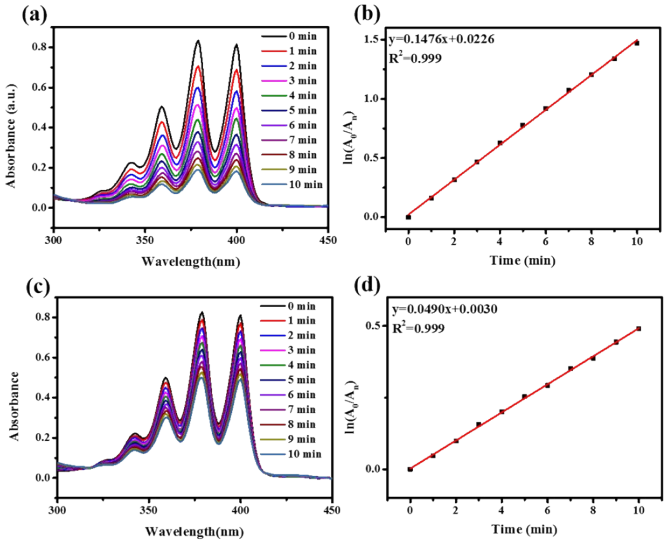

Fig. S18 (a) UV-Vis spectra of ABDA (20 μM) with RB in PBS under laser irradiation (532 nm, 0.01 W cm^{-2}). (b) The absorbance decay of ABDA at 378 nm in PBS under laser irradiation (532 nm, 0.01 W cm^{-2}) with RB. (c) UV-Vis spectra of ABDA (20 μM) with CCN in PBS under laser irradiation (532 nm, 0.01 W cm^{-2}). (d) The absorbance decay of ABDA at 378 nm in PBS under laser irradiation (532 nm, 0.01 W cm^{-2}) with CCN.

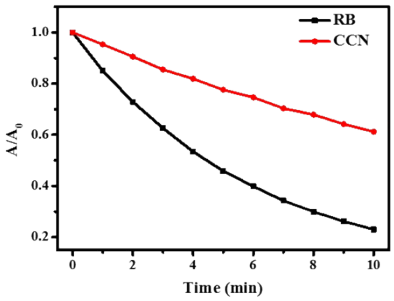

Fig. S19 The degradation rate of ABDA at 378 nm in the presence of RB and CCN under laser irradiation (532 nm, 0.01 W cm^{-2}).

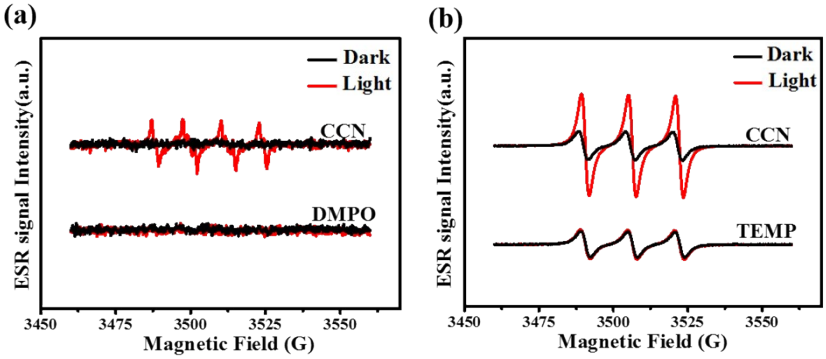

Fig. S20 ESR signals of (c) $O_2^{\bullet-}$ and (d) $^1O_2$ of CCN under laser irradiation (532 nm, 0.01 W cm^{-2}).

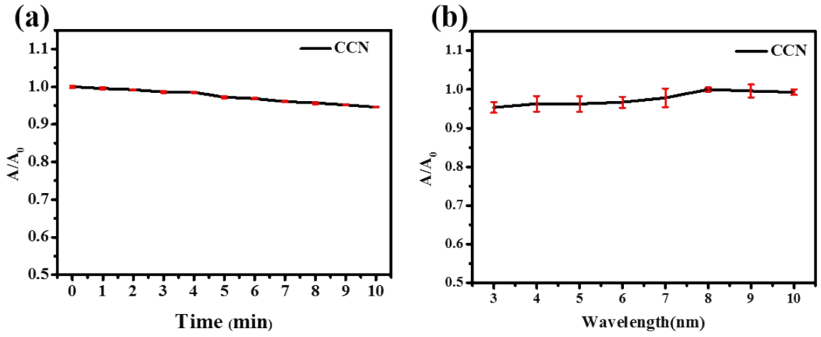

Fig. S21 (a) Photostability (A/A_0) of CCN at 537 nm under laser irradiation (532 nm, 0.05 W cm^{-2}). (b) pH Stability (A/A_0) of CCN at 537 nm in PBS with pH 3.0, 4.0, 5.0, 6.0, 7.0, 8.0, 9.0, 10.0.

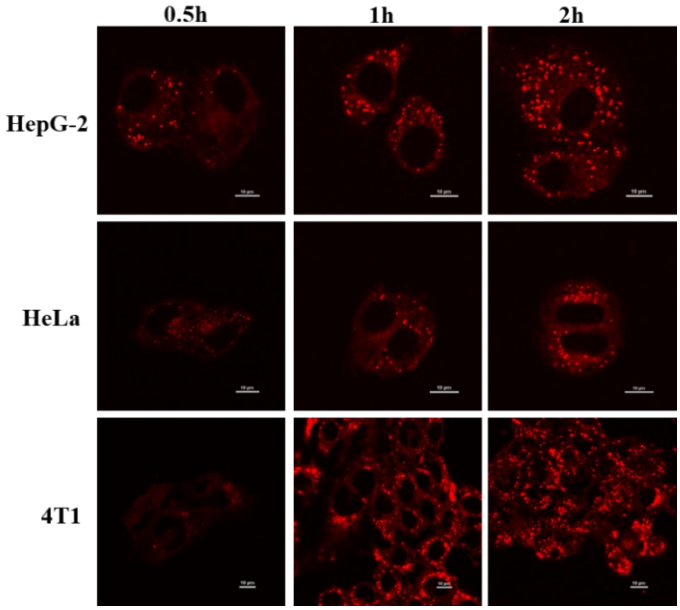

Fig. S22 CLSM images of HepG-2, HeLa and 4T1 cells after treatment with CCN (2 μM). Scale bar: 10 μm.

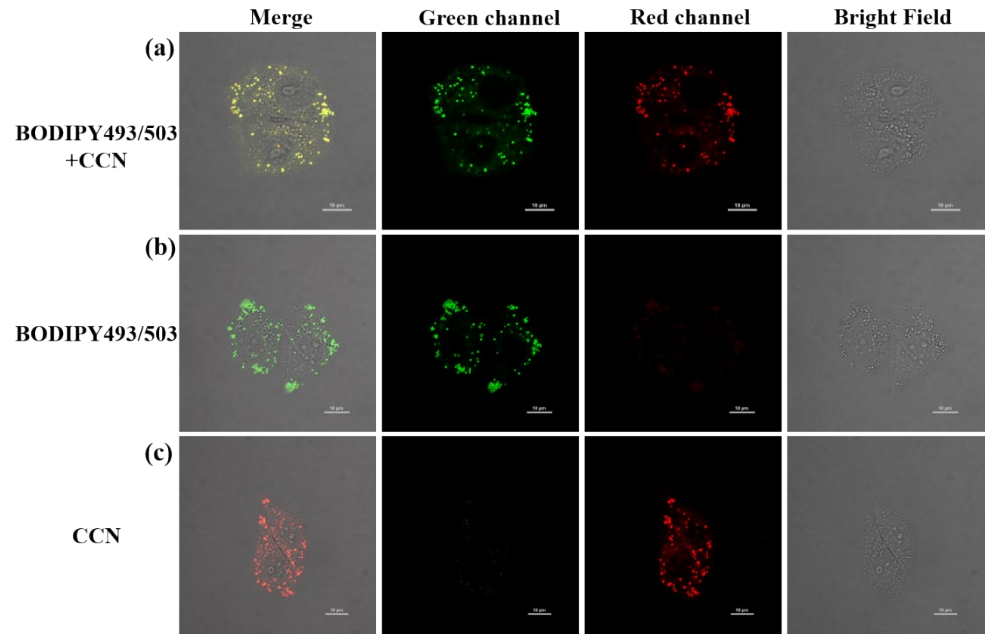

Fig. S23 CLSM images of (a) BODIPY (0.5 μM) and CCN (2 μM), (b) BODIPY, (c) CCN (2 μM) in HepG-2 cells. Scale bar: 10 μm

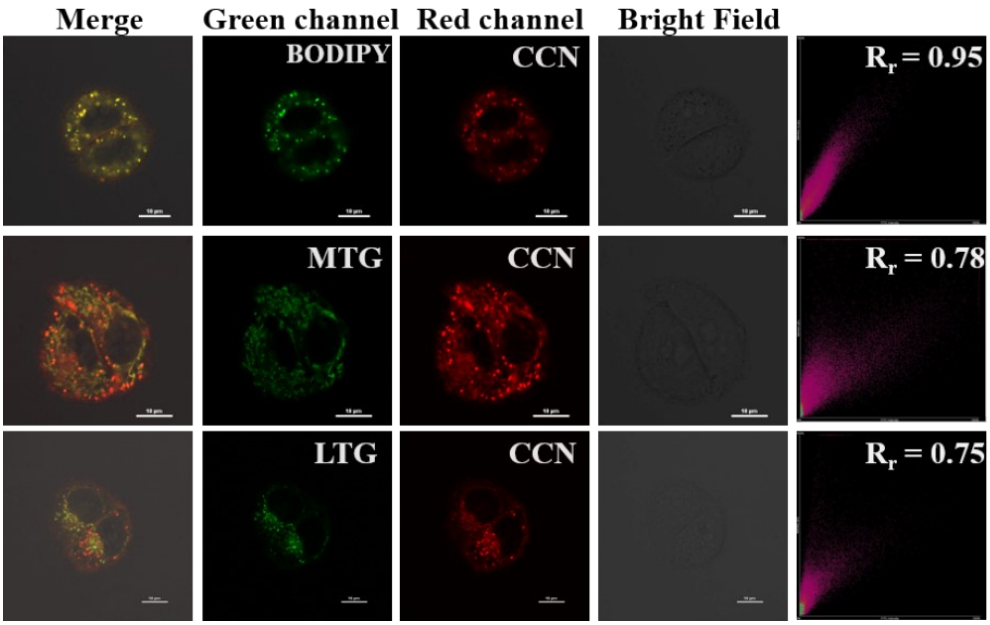

Fig. S24 CLSM images of CCN (2 μM) colocalized with BODIPY (0.5 μM), MTG (0.2 μM), LTG (0.2 μM) in HeLa cells. Scale bar: 10 μm.

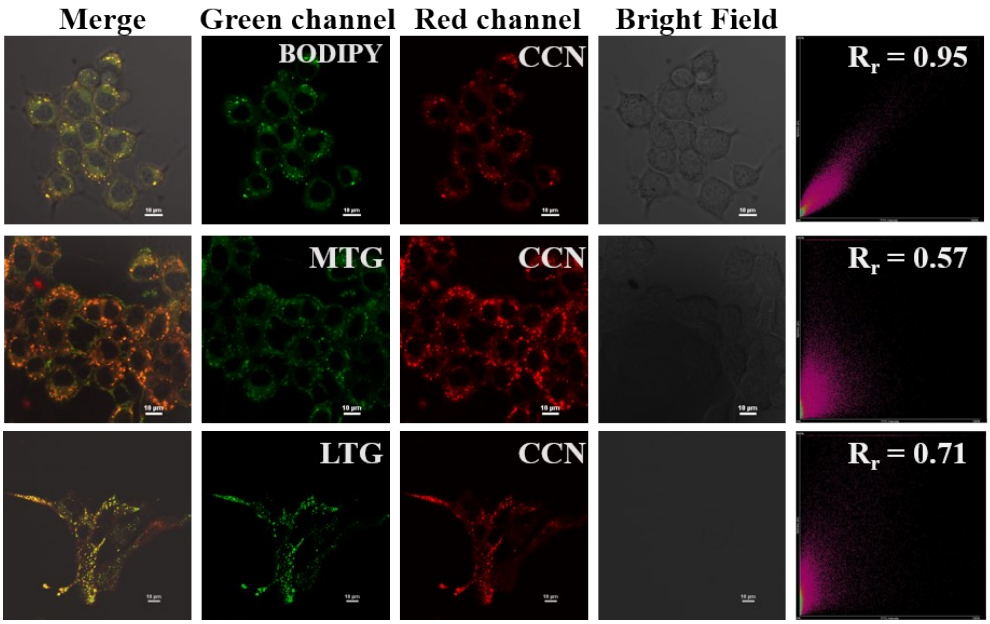

Fig. S25 CLSM images of CCN (2 μM) colocalized with BODIPY (0.5 μM), MTG (0.2 μM), LTG (0.2 μM) in 4T1 cells. Scale bar: 10 μm.

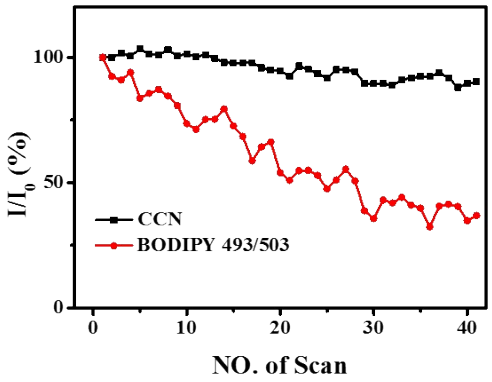

Fig. S26 Loss of emission intensity (I/I_0) of CCN (2 μM) and BODIPY (0.5 μM) in HepG-2 cells with the increasing irradiation time.

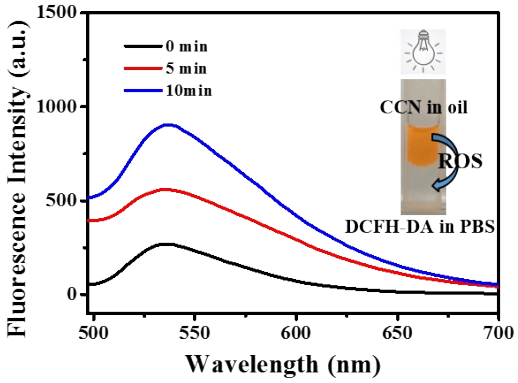

Fig. S27 Spectral simulation of ROS transfer from LDs to cytoplasmic matrix.

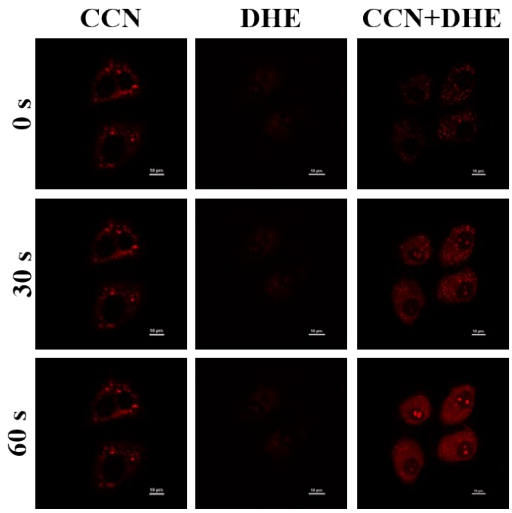

Fig. S28 CLSM images of HepG-2 cells after being incubated with CCN (2 μM) and loaded with DHE (10 μM) in normoxia under laser irradiation (532 nm, 0.02 W cm^{-2}). Scale bar: 10 μm.

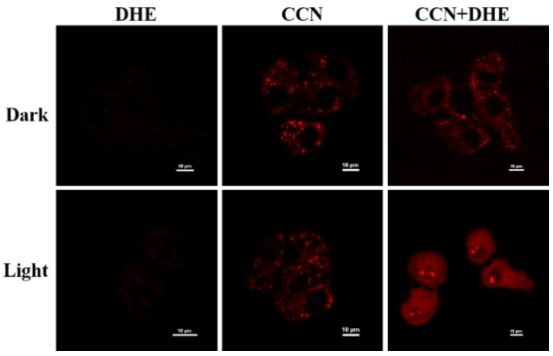

Fig. S29 CLSM images of HepG-2 cells after being incubated with CCN (2 μM) and loaded with DHE (10 μM) in hypoxia under laser irradiation (532 nm, 0.02 W cm^{-2}) for 1 min. Scale bar: 10 μm.

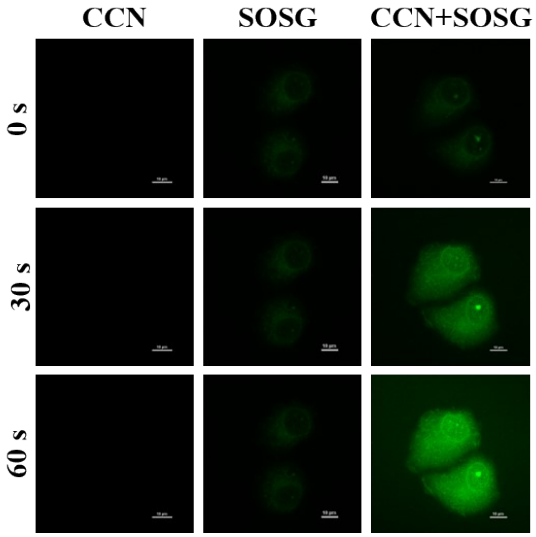

Fig. S30 CLSM images of HepG-2 cells after being incubated with CCN (2 μM) and loaded with SOSG (5 μM) in normoxia under laser irradiation (532 nm, 0.02 W cm^{-2}).Scale bar: 10 μm.

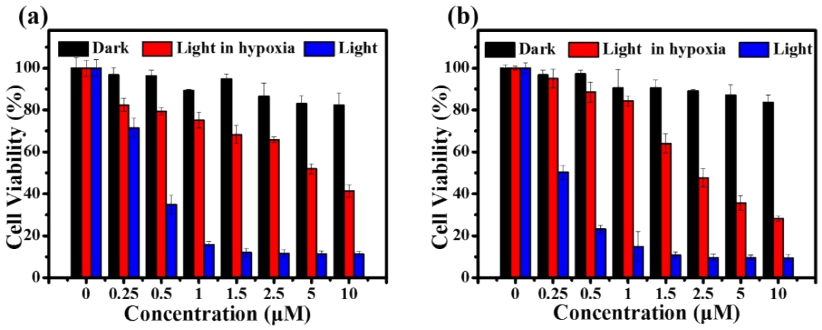

Fig. S31 Cell viability of (a) HeLa and (b) 4T1 cells after being incubated with different concentrations of CCN with irradiation of 532 nm laser (0.1 W cm^{-2}) for 10 min.

Table S4 The calculated IC50 of CCN for HepG-2, HeLa, and 4T1 cells.

	Phototoxicity in Normoxia (μM)	**Phototoxicity in Hypoxia (μM)**	**Dark cytotoxicity (μM)**
HepG-2	0.99	8.58	105.09
HeLa	0.50	6.87	100.63
4T1	0.41	3.30	82.14

Notes and references

1. Y. Zhang, H. Teng, Y. Gao, M. W. Afzal, J. Tian, X. Chen, H. Tang, T. D. James and Y. Guo, *Chin. Chem. Lett.*, 2020, **31**, 2917-2920.
2. J. Ma, R. Sheng, J. Wu, W. Liu and H. Zhang, *Sens. Actuators B: Chem.*, 2014, **197**, 364-369.
3. J. Fan, H. Cai, Q. Li, Z. Du and W. Tan, *J Biotechnol*, 2012, **158**, 104-111.
4. J. Ge, M. Lan, B. Zhou, W. Liu, L. Guo, H. Wang, Q. Jia, G. Niu, X. Huang, H. Zhou, X. Meng, P. Wang, C. S. Lee, W. Zhang and X. Han, *Nat. Commun*,. 2014, **5**, 4596.
5. J. Sun, K. Du, J. Diao, X. Cai, F. Feng and S. Wang, *Angew Chem. Int. Ed.*, 2020, **59**, 12122-12128.